ROYAL SOCIETY
OF CHEMISTRY

PAPER

Check for updates

Real-time analysis and prediction method of ion concentration using the effect of O–H stretching bands in aqueous solutions based on ATR-FTIR spectroscopy†

So Hyun Baek,‡[ab] Jeungjai Yun,‡[ac] Seung-Hwan Lee,[a] Hyun-Woo Lee,[a] Yongbum Kwon,[a] Kee-Ryung Park,[a] Yoseb Song,[a] Bum Sung Kim,[a] Rhokyun Kwak,[c] Haejin Hwang[b] and Da-Woon Jeong [ID] *[a]

Analyzing the concentration of ions in aqueous solutions in real-time plays an important role in the fields of chemistry and biology. Traditional methods for measuring ion concentrations, such as concentration analysis by measuring electrical conductivity, inductively coupled plasma mass spectrometry, and ion chromatography, have been used in many research fields. However, these methods are limited in determining ion concentrations instantaneously. Fourier-transform infrared-attenuated total reflectance (ATR-FTIR) spectroscopy provides a new approach for determining ion concentrations in aqueous solutions. This allows for fast analysis without pretreatment and is scalable for real-time measurements. In this study, we present a method for measuring ion concentrations by examining ion–water interactions in the O–H stretching band of aqueous solutions using ATR-FTIR spectroscopy. Five aqueous solutions, namely LiCl + HCl, LiOH + HCl, LiOH, Li_3PO_4, and NaCl were used in the experiments and prepared at concentrations between 0.5–2 M. The ion concentrations in the prepared aqueous solutions were measured using ATR-FTIR spectroscopy. We observed that the difference in absorbance increased and decreased linearly with changes in concentration. The concentration of ions in the aqueous solution could be measured by validating the designed linear regression analysis function model. In this study, we proposed five linear regression analysis function models, all of which showed high coefficients of determination above 0.9, with the highest coefficient of determination reaching 0.9969. These results show that ATR-FTIR spectroscopy has the potential to be applied as a rapid and simple concentration analysis system.

1. Introduction

Instantaneous determination of ion concentrations in aqueous solutions is a crucial analytical technique used in various fields. In industries, measuring ion concentrations in aqueous solutions, whether crude or diluted, is an important indicator of reliability and production control.[1,2] Accurate analysis of dissolved ion concentrations provides decisive information for chemistry, drug development,[3] environmental monitoring,[4,5]

and studies on biological interactions,[6] enhancing their practical applications. In areas of recent extensive research, such as seawater desalination and the ionic enrichment of water-soluble resources, predicting ion concentrations simply and instantaneously proves effective for overall system management.[4,5]

Conventional methods for measuring ion concentrations include electrical conductivity (EC) measurements, inductively coupled plasma mass spectrometry (ICP-MS), and ion chromatography (IC). Although these methods have been successfully used in many basic research applications, they have several limitations in terms of accuracy, sensitivity, selectivity, and the ability to measure multiple ions simultaneously.[1–10] EC measurement is considered an effective tool for seawater desalination and analyzing changes in ion concentrations. This method can easily provide real-time measurements of ion concentrations in a solution, which is crucial for seawater desalination. However, this method employs a conductivity meter that measures the electrical conductivity of an aqueous

[a]*Department of Korea National Institute of Rare Metals, Korea Institute of Industrial Technology, Incheon 21655, Republic of Korea. E-mail: dwjeong@kitech.re.kr; Fax: +82-32-226-1374; Tel: +82-32-226-1362*

[b]*Department of Material Science Engineering, Inha University, Incheon 22212, Republic of Korea*

[c]*Department of Mechanical Convergence Engineering, Hanyang University, Seoul 04763, Republic of Korea*

† Electronic supplementary information (ESI) available. See DOI: https://doi.org/10.1039/d4ra01473a

‡ So Hyun Baek and Jeungjai Yun contributed equally to this work.

solution, which cannot distinguish between individual ions and has limitations in high-resolution and simultaneous multi-ion measurements.[5,8–10] ICP-MS is known for its excellent sensitivity and ability to measure multiple ions simultaneously. Moreover, its high-resolution spectra enable the precise analysis of ions in a variety of compounds. However, this method is limited by its relatively high cost, complex operation and maintenance, and lack of sensitivity to certain compounds.[11] IC is recognized as a powerful method for separating and quantitatively measuring ions. However, it requires long analysis times, including pretreatment, and has limitations in detecting certain ions.[12] The Fourier-transform infrared-attenuated total reflectance (ATR-FTIR) spectroscopy method presented in this study provides an innovative approach for analyzing ion concentrations in aqueous solutions. This method utilizes the transmission, reflection, and absorption of IR radiation, and the measurement of ion concentrations can be modularized and directly applied to the sample. In addition, ATR-FTIR spectroscopy works effectively in a wide range of solvents, including water, allowing its application in various environments without the need for pretreatment. Furthermore, this system can be expanded by equipping the instrument with an attenuated total reflection (ATR) module to observe real-time changes in concentration.[13–15] With these advantages, the ATR-FTIR spectroscopy method offers a new integrated and efficient solution for analyzing ion concentrations in pre-purified samples or complex matrices[11,16–25] (Fig. 1).

Ion concentration analysis *via* ATR-FTIR spectroscopy uses the inherent absorbance properties of the O–H functionality.[11,13] This method is an internal reflection technique, and the absorbance of the O–H stretching band is used to determine the ion concentration in an aqueous solution. O–H stretching bands are mainly observed in the 3000–3700 cm^{-1} range.[11] Because these bands exhibit specific frequencies and peak shapes depending on their interactions with different ionic species in aqueous solutions, unique chemical information can be obtained through ATR-FTIR spectroscopy.[26–29] These characteristics suggest the potential of ATR as a useful tool for analyzing ion concentrations in aqueous solutions because it can sensitively detect interactions between compounds and the chemical state of a substance. A key characterization parameter for seawater desalination using electrodialysis is the rate of removal of salts contained in the pre-desalination solution. This rate is determined primarily by the decrease in the electrical conductivity of the post-desalination solution. Thus, it is difficult to detect changes in the concentration of certain ions in solution using EC measurements. In addition, the electrodes used for EC measurements can be noisy because of the effects of the electrodialysis electric field.[5,8–10] As an optical method, ATR-FTIR spectroscopy minimizes the effects of the solution and electric field and enables the immediate and continuous analysis of the concentration behavior in the solution. ATR-FTIR spectroscopy has been used to study the shift of O–H stretching bands by dissolved substances.[30,31]

The correlation between ion concentrations and the absorbance of O–H stretching bands is key for understanding and analyzing the chemical properties of compounds. O–H stretching bands appear at specific frequencies and exhibit specific peak shapes, which fluctuate depending on the state of the O–H bond of the water molecule.[11,16–25] When the
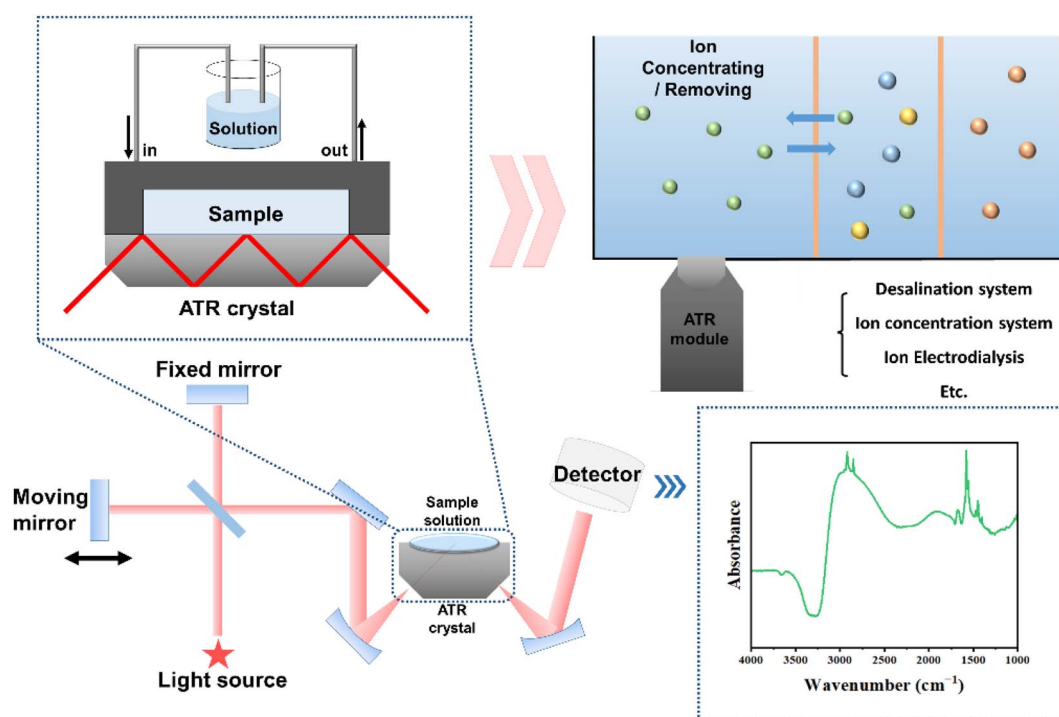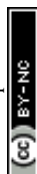

Fig. 1 Schematic diagrams of ATR–FTIR measurement principle and its application to various aqueous ion systems.

concentration of an ion in an aqueous solution increases, its interaction with the surrounding water molecules increases, resulting in a change in the absorbance of the O–H stretching band. Therefore, ATR-FTIR spectroscopy can be used to obtain uniquely useful information by detecting and tracking changes in ion concentrations through the absorbance measurements of O–H stretching bands.

In this study, an ATR-FTIR spectroscopy method was used to measure the concentration of ions in an aqueous solution by analyzing the ion–water interactions of the O–H stretching bands. For this purpose, 0.5–2.0 M solutions of LiCl + HCl, LiOH, LiOH + H_3PO_4, LiOH + HCl, and NaOH + HCl were prepared, and their ion concentrations were measured using ATR-FTIR spectroscopy. The differences in the absorbance of the aqueous solutions were analyzed with changes in ion concentrations.

2. Experimental

2.1. Chemicals

The reagents used for preparing the aqueous solutions were lithium hydroxide (LiOH, 98.0%, Sigma-Aldrich), lithium chloride (LiCl, 99.0%, Sigma-Aldrich), hydrochloric acid (HCl, 35.0%, DAEJUNG), and phosphoric acid (H_3PO_4, 85.0%, DAEJUNG). In addition, 99.9% pure water was used as the solvent for preparing the aqueous solutions.

2.2. Preparation of standard and test solutions

In analytical chemistry, the matrix effect refers to the influence of components of a sample matrix on the detection or quantitation of the analyte. It is mainly caused by chemical interference or background noise. Therefore, in analytical chemistry, minimizing the matrix effect is important to improve reliability. In this study, samples were prepared by adjusting the mixing ratio such that only the concentration of a particular ion acted as a variable, considering the matrix effect because both cations and anions present in aqueous solutions can affect the O–H stretching band of water. It is important to minimize the influence of the components of the sample matrix on the detection or quantification of the analyte because this can degrade the accuracy of the analytical results. The variable in this experiment was the concentration of cations Li^+ and Na^+ (0.5–2.0 M), which minimized the effect of anions. In addition, to eliminate the effect of the concentration of a single anion such as Cl^- on the results, the sample was prepared by strictly controlling the mixing ratio of the added solutions, as listed in Table 1. In addition, to eliminate background noise, the water used as a solvent was set to background and the experiment was performed after its removal to minimize any matrix effect that may occur in this study.

LiOH and LiCl powders and HCl and H_3PO_4 solutions were weighed and mixed in a conical tube. Approximately 8 mL of pure water was added to the tube. Afterwards, the tubes were placed in a bath sonicator for 30 min to completely dissolve the powder. After dissolving the powder in a solvent, pure water was added to adjust the final solution volume to 10 mL, and

Table 1 Preparation parameters of the sample solutions

Test	Solutions	Solutes	Molarity (M)			
1	LiCl	LiCl	0.5	1	1.5	2
		HCl	1.5	1	0.5	0
2	LiOH	LiOH	0.5	1	1.5	2
		H_2O	—	—	—	—
3	Li_3PO_4	LiOH	0.5	1	1.5	2
		H_3PO_4	3	3	3	3
4	LiCl	LiOH	0.5	1	1.5	2
		HCl	3	3	3	3
5	NaCl	NaOH	0.5	1	1.5	2
		HCl	3	3	3	3

a homogeneous solution was obtained using a bath sonicator for 30 seconds. The prepared solution was covered to prevent evaporation.

2.3. ATR-FTIR measurements

An ATR (ZnSe) module connected to a Fourier-transform infrared spectrophotometer (Spectrum Two, PerkinElmer) was used. The ATR technique utilizes the ATR phenomenon, which occurs when the angle of incidence is greater than the critical angle, and light travels from a medium with a high refractive index to a medium with a lower refractive index. In this case, not all of the light is reflected; instead, some light penetrates the upper medium, forming an evanescent wave. When the sample absorbs the evanescent wave, the intensity of light in the total reflection is reduced, enabling the measurement of the degree of absorption at a certain wavelength.

First, the surface of the ATR stage was cleaned using pure water. To set the background to water as the solvent, a drop of pure water was placed on the measurement window of the ATR module to measure the background data. Next, the prepared sample was placed on the measurement window to measure the absorbance as a function of wavenumber. The amount of sample solution used was 100 μL, and the measurement was repeated five times to eliminate errors. The PerkinElmer Spectrum software was used, and the wavenumber range was set to 600–4000 cm^{-1}; the results were calculated by repeating the measurement five times for each condition.

The modified absorbance was introduced to effectively observe changes in absorbance by setting the starting and ending points to zero in the O–H stretching band region (3000–3700 cm^{-1}). This graphing technique enhances the visualization of data variability, facilitating easier identification of concentration-dependent changes and more distinctly delineating trends. It is crucial in this process to ensure that the trends in the graph remain unaltered. Careful attention was paid during the modification of the graph to prevent distortion of the data and maintain the integrity of the trends. The modified absorbance graph thus ensures the reliability of the results, preserving the characteristics of the original data without further modification. This method provides consistency and reliability in the data analysis process.

3. Results and discussion

The difference in the ATR absorbances of the mixed solutions was analyzed based on cation concentration. Fig. 2a and b show the graphs of absorbance as a function of wavenumber measured using the ATR-FTIR spectroscopy of LiCl (LiCl + HCl) and LiOH (LiOH + H_2O) solutions with molar concentrations of cations (Li^+) in the 0.5–2 M range. In this case, the anions paired with Li^+ were fixed as Cl^- and OH^-. In addition, both graphs show the various shapes of O–H stretching bands in the broad wavenumber region of 600–4000 cm^{-1}. The bands in the graphs of the same solute show differences in absorbance depending on its concentration in the solution; however, the shapes of these graphs are the same. In contrast, the bands for different solutions show distinct shapes. In this study, we analyzed the concentration dependence on the difference in absorbance of the O–H stretching band at 3300 cm^{-1}. This dependence can be clearly observed in the graphs with modified absorbance in the concentrated wavenumber region of Fig. 2c and d. As shown in Fig. 2c, the intensity of the absorbance increases linearly with the concentration of Li^+ in the LiCl solution. This relationship was confirmed using the linear regression fit in Fig. 2e. The
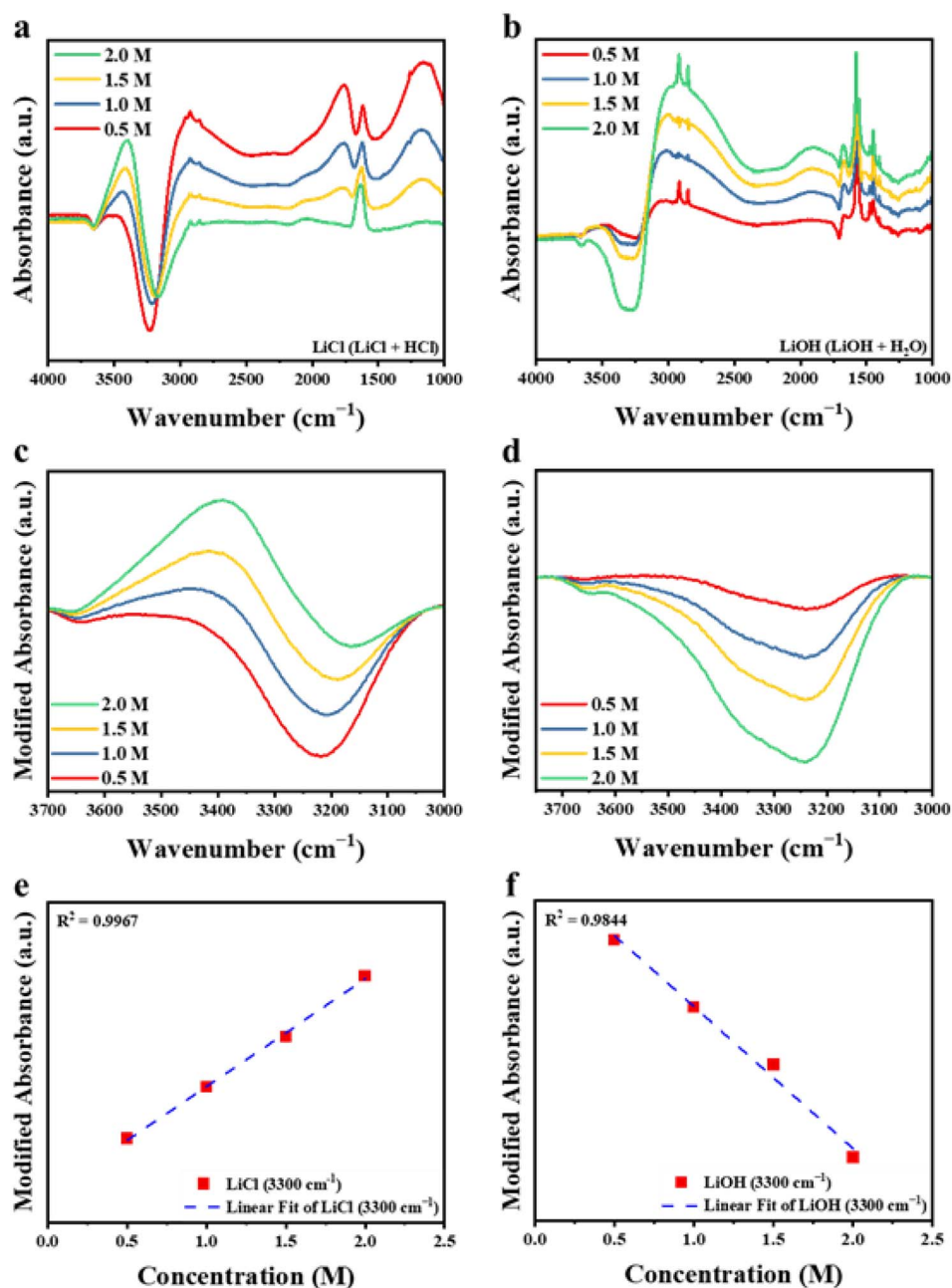

Fig. 2 (a and b) ATR-FTIR absorbance of the LiCl (LiCl + HCl) and LiOH (LiOH + H_2O) solutions depending on the molarity of the cation. (c and d) Differences in the absorbance of the O–H stretching band at 3300 cm^{-1} in LiCl (LiCl + HCl) and LiOH (LiOH + H_2O) solutions based on cation (Li^+) molarity. (e and f) Linear regression analysis function graphs of absorbance based on the cation molarity in (c and d).

linearity of the absorbance increase was demonstrated by linear regression analysis using a quadratic function, where the coefficient of determination (R^2) was 0.9967. This value indicates a high accuracy of more than 0.9. However, in the LiOH (LiOH + H_2O) solution Fig. 2d, the absorbance decreased linearly with increasing molarity of Li^+. The results for the LiOH (LiOH + H_2O) solution Fig. 2f show this difference as a function of the linear regression analysis. In this case, the graph had a negative slope, confirming the high accuracy with an R^2 of 0.9844. In the above experiment, the concentrations of counter anions such as PO_4^- and Cl^-, except Li^+, in the experimental solution were controlled equally; therefore, this linear increase in absorbance could be because of the concentration dependence of Li^+.

As shown in Fig. 3, when the two solutes used in the mixed solution do not contain the same anion, the absorbance difference in the O–H band region of the cations shows a concentration dependence on Li^+. Fig. 3a–c show the ATR-FTIR graphs of Li_3PO_4 (LiOH + H_3PO_4), LiCl (LiOH + HCl),

and NaCl (NaOH + HCl) solutions, respectively. Similar to previous results, identical band shapes were observed in the graphs of the solutions containing the same solutes, while distinct band shapes were observed for solutions containing different solutes. Fig. 3d–f show a difference in absorbance in the O–H stretching band region with increasing Li^+ concentration. Notably, the absorbance increased or decreased linearly with concentration, and we plotted it using a linear regression function in Fig. 3g–i. All three models were highly accurate, with R^2 values above 0.9. Although a small experimental error was noted in the 1 M Li_3PO_4 solution, it did not significantly affect the linear function model.

Using the linear regression analysis functions shown in Fig. 2e, f, and 3, a quadratic function model, the linear regression analysis function (LRAF) model was developed and is presented in Table 2. This model can predict the molar concentration of cations (Li^+ and Na^+) based on the absorbance measurements of each mixed solution. The anionic species of
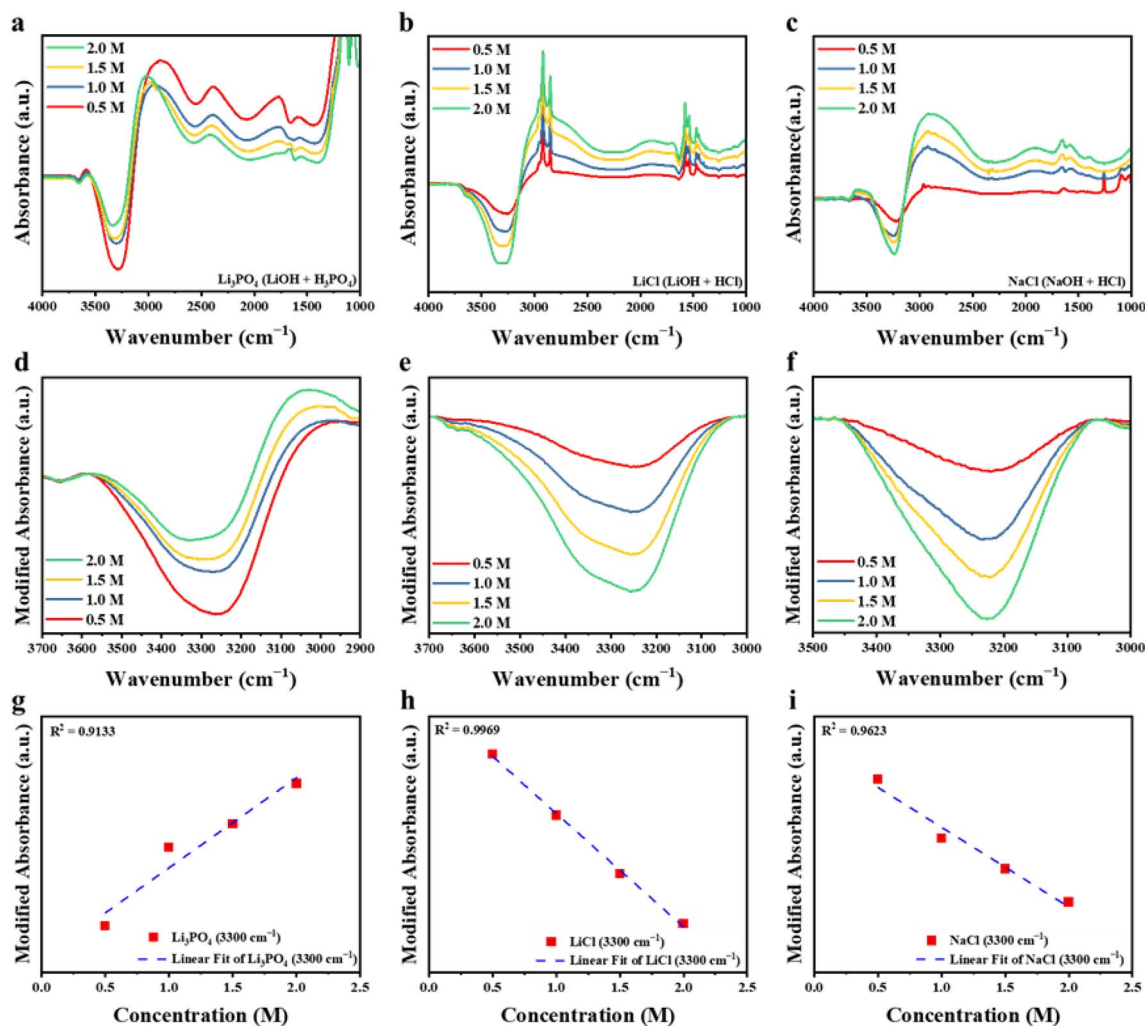

Fig. 3 (a–c) ATR-FTIR absorbance of the Li_3PO_4 (LiOH + H_3PO_4), LiCl (LiOH + HCl), and NaCl (NaOH + HCl) solutions depending on the molarity of Li^+ and Na^+ cations. (d–f) Differences in the absorbance of the O–H stretching band at 3300 cm^{-1} in Li_3PO_4 (LiOH + H_3PO_4), LiCl (LiOH + HCl), and NaCl (NaOH + HCl) solutions based on cation (Li^+ and Na^+) molarity. (g–i) Linear regression analysis function graphs of absorbance based on the cation molarity in (d–f).

Table 2 Molarity calculations based on LRAF models and the adjusted coefficients of determination $(R^2)^a$

Test	Solutions	Solutes	Linear regression analysis function models	Adjusted coefficient of determination (R^2)
1	LiCl	LiCl	$y = 45.79x + 1.57$	0.9967
		HCl		
2	LiOH	LiOH	$y = -56.31x + 0.25$	0.9844
		H_2O		
3	Li_3PO_4	LiOH	$y = 70.82x + 3.39$	0.9133
		H_3PO_4		
4	LiCl	LiOH	$y = -48.83x - 0.09$	0.9969
		HCl		
5	NaCl	NaOH	$y = -116.55x - 0.10$	0.9623
		HCl		

^{a} y: Calculated molarity, x: absorbance.

the solutes in the mixed solution affected the absorbance of O–H stretching band and hence determined the sign of the slope of the LRAF. The LiCl solution in Test 1 contained no OH^- ions; therefore, LRAF 1 exhibits a positive slope. However, in Tests 2, 4, and 5, the solutions contained either OH^- ions or a mixture of OH^- and Cl^- ions; therefore, the LRAF graphs of Tests 2, 4, and 5 show a negative slope. This suggests that, between the monovalent anions OH^- and Cl^-, the effect of OH^- anions on the absorbance of the O–H stretching is dominant. In Test 3, both OH^- and PO_4^{3-} anions were present in the solvent. However, LRAF 3 exhibits a positive slope, confirming the dominant effect of the trivalent PO_4^{3-} anion.

To validate the LRAF model, a test solution of 1.3 M Li_3PO_4 was prepared, and its molarity was analyzed using the LRAF 3 model. Fig. 4a shows a graph of the ATR-FTIR absorbance of the test solution, followed by the baseline fitting of the O–H stretching band area. The absorbance value at 3300 cm^{-1} was then substituted into the LRAF 3 model to predict a molarity value of 1.35 M. This process is illustrated in Fig. 4b. The predicted value of 1.35 M has an error of 4.05% for the actual value of 1.3 M, which is very low (less than 5%) and does not exceed

the error range of ±4.34% for LRAF 3. However, this error indicates that the proposed concentration prediction model cannot be used as a precise measurement method. This is because the cations and anions in aqueous solutions have complex effects on the O–H stretching bands. In addition, owing to the very low viscosity of aqueous solutions and the nature of ATR-FTIR spectroscopy, the absorbance measurements are highly dependent on the measurement ability of the operator. Despite these limitations, the rapid, simple measurement method and low cost of measurement make the model proposed in this study useful. In addition, this noncontact spectroscopy method can be developed into a continuous concentration prediction system through modularization expansion and combination with an aqueous solution bath.

Furthermore, to explore the potential of a multivariate model, we conducted PLS (Partial Least Squares) regression analysis using mixed solutions and the experimental details regarding the PLS regression analysis is given in the ESI (Table S1).† These mixed solutions exhibited trends depending on their concentrations (Fig. S1†). Although the LiCl 1 M + NaCl 2 M and LiCl 2 M + NaCl 1 M solutions have different
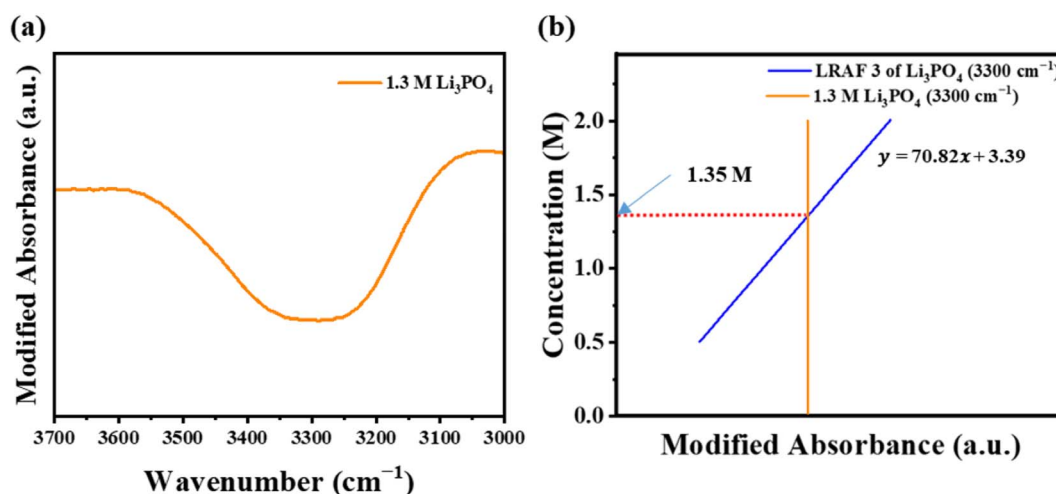

Fig. 4 (a) Absorbance of the 1.3 M Li_3PO_4 (LiOH + H_3PO_4) solution in the O–H stretching band range (3000–3700 cm^{-1}). (b) Molarity calculated by LRAF 3 for Li_3PO_4 (3300 cm^{-1})

Paper

concentrations, they exhibited only slight differences owing to their equal total concentration. After observing these trends, we performed the Fourier self-deconvolution peak analysis for detailed analysis. As shown in Fig. S2,† the peaks of Li^+ and Na^+ were separately compared, revealing a correlation wherein the intensity of the peaks increased proportionally to the ionic concentrations. However, the two ions exhibited mutual interference, complicating the separate analysis. Evidently, for multivariate analysis, complex factors such as cations and anions must be considered. Further studies are required to construct an effective multivariate model by building a comprehensive database and integrating PLS regression with Fourier self-deconvolution peak-analysis methods.

4. Conclusions

In this study, we developed a rapid, simple, and economical method for determining target ion concentrations in aqueous solutions using ATR-FTIR spectroscopy. We observed that hydrated ions in aqueous solutions affect the binding force of the O–H stretching band. In addition, the difference in the absorbance shows linearity with both increasing and decreasing molar concentrations of a particular ion within the range of 0.5 to 2.0 M. Although the presence of cations and anions compoundedly affects the ATR absorbance of the solution, the linearity between absorbance and the target ion concentration in the O–H stretching band region at 3300 cm^{-1} is sufficiently accurate (coefficient of determination $R^2 \geq 90$) to establish a linear regression model. The LRAFs for the five solutions were developed based on these linear regression analyses.

By validating the proposed LRAF model, the molarity of a 1.3 M test solution was found to be 1.35 M with a low error value of 4.05%. Therefore, this tool is more suitable for qualitative concentration predictions rather than for highly precise concentration measurements. Extending the LRAF model through further experiments will facilitate the prediction of ion concentrations in aqueous solutions containing a mixture of various ions. With this scaled-up process, the proposed ion concentration prediction model has the potential to be utilized in various industries, including seawater desalination plants, ion recovery plants for aqueous solutions, and waste treatment facilities.

Data availability

The data supporting this article have been included as part of the ESI.†

Author contributions

So Hyun Baek: data curation, validation visualization and writing – original draft. Jeungjai Yun: formal analysis, writing – original draft. Seung-Hwan Lee: data curation, methodology. Hyun-Woo Lee: methodology, data curation. Yongbum Kwon: formal analysis, methodology. Kee-Ryung Park: software, validation. Yoseb Song: conceptualization, formal analysis. Bum Sung Kim: supervision, validation. Rhokyun Kwak: supervision,

formal analysis. Haejin Hwang: supervision, methodology. Da-Woon Jeong: supervision, writing – review & editing, project administration and funding acquisition.

Conflicts of interest

The authors declare that they have no known competing financial interests or personal relationships that could have appeared to influence the work reported in this paper.

Acknowledgements

References

1 R. Falciai, A. Mignani and A. Vannini, *Sens. Actuators, B*, 2001, **74**, 74–77.
2 K. Masuda, T. Haramaki, S. Nakashima, B. Habert, I. Martinez and S. Kashiwabara, *Appl. Spectrosc.*, 2003, **57**, 274–281.
3 S. T. Hassib, G. S. Hassan, A. A. El-Zaher, M. A. Fouad and E. A. Taha, *Spectrochim. Acta, Part A*, 2017, **186**, 59–65.
4 D. Curto, V. Franzitta and A. Guercio, *Appl. Sci.*, 2021, **11**, 670.
5 D. Kim, S. Ihm, S. Park, Y. Yu and R. Kwak, *Desalination*, 2021, **499**, 114810.
6 S. J. Kim, S. H. Ko, K. H. Kang and J. Han, *Nat. Nanotechnol.*, 2010, **5**, 297–301.
7 N. M. P. de Souza, B. H. Machado, L. V. Padoin, D. Prá, A. P. Fay, V. A. Corbellini and A. Rieger, *Talanta*, 2023, **254**, 123858.
8 M. Y. Thompson, D. Brandes and A. D. Kney, *J. Environ. Manage.*, 2012, **104**, 152–157.
9 C. Chang, T. Sommerfeldt, J. Carefoot and G. Schaalje, *Can. J. Soil Sci.*, 1983, **63**, 79–86.
10 M. Hayashi, *Environ. Monit. Assess.*, 2004, **96**, 119–128.
11 N. Kitadai, T. Sawai, R. Tonoue, S. Nakashima, M. Katsura and K. Fukushi, *J. Solution Chem.*, 2014, **43**, 1055–1077.
12 D. Li, W. Huang and R. Huang, *J. Hazard. Mater.*, 2023, 131952.
13 E. V. Solovyeva, H. Lu, G. A. Khripoun, K. N. Mikhelson and S. G. Kazarian, *J. Membr. Sci.*, 2021, **619**, 118798.
14 I. C. Stefan, D. Mandler and D. A. Scherson, *Langmuir*, 2002, **18**, 6976–6980.
15 L. T. Cuba-Chiem, L. Huynh, J. Ralston and D. A. Beattie, *Miner. Eng.*, 2008, **21**, 1013–1019.
16 L. C. Lee, C.-Y. Liong and A. A. Jemain, *Chemom. Intell. Lab. Syst.*, 2017, **163**, 64–75.
17 L. J. Kirwan, P. D. Fawell and W. van Bronswijk, *Langmuir*, 2004, **20**, 4093–4100.

18 A. R. Hind, S. K. Bhargava and A. McKinnon, *Adv. Colloid Interface Sci.*, 2001, **93**, 91–114.

19 Y. Furutani, H. Shimizu, Y. Asai, T. Fukuda, S. Oiki and H. Kandori, *J. Phys. Chem. Lett.*, 2012, **3**, 3806–3810.

20 T. Lindfors, F. Sundfors, L. Höfler and R. E. Gyurcsányi, *Electroanalysis*, 2009, **21**, 1914–1922.

21 Z.-F. Wei, Y.-H. Zhang, L.-J. Zhao, J.-H. Liu and X.-H. Li, *J. Phys. Chem. A*, 2005, **109**, 1337–1342.

22 L. Meyer, D. Curran, R. Brow, S. Santhanagopalan and J. Porter, *J. Electrochem. Soc.*, 2021, **168**, 090502.

23 R. Prasad, S. H. Crouse, R. W. Rousseau and M. A. Grover, *Ind. Eng. Chem. Res.*, 2023, **62**, 15962–15973.

24 T. Togkalidou, M. Fujiwara, S. Patel and R. D. Braatz, *J. Cryst. Growth*, 2001, **231**, 534–543.

25 E. P. Kovalev, S. A. Prikhod'ko, A. S. Shalygin and O. N. Martyanov, *Mendeleev Commun.*, 2023, **33**, 425–427.

26 W. RonaldáFawcett, *J. Chem. Soc., Faraday Trans.*, 1994, **90**, 2697–2701.

27 J. Cornel, C. Lindenberg and M. Mazzotti, *Ind. Eng. Chem. Res.*, 2008, **47**, 4870–4882.

28 P. Roonasi and A. Holmgren, *J. Colloid Interface Sci.*, 2009, **333**, 27–32.

29 L. Sim, S. Gan, C. Chan and R. Yahya, *Spectrochim. Acta, Part A*, 2010, **76**, 287–292.

30 A. G. Al Lafi, *Polym. Degrad. Stab.*, 2014, **105**, 122–133.

31 R. E. Masithoh, F. Roosmayanti, K. Rismiwandira and M. F. R. Pahlawan, *Sugar Tech*, 2022, **24**, 920–929.